

Effects of the growth conditions on domain wall motion in Pt/Co/Pt stacks

C.P. Quinteros,^{1, a)} M.J. Cortés Burgos,^{2,3} L.J. Albornoz,^{2,3,4} S. Bustingorry,² J. Gómez,² P. Granell,⁵ F. Golmar,⁶ M.L. Ibarra,^{7,8} J. Curiale,^{2,3} and M. Granada²

¹⁾*Zernike Institute for Advanced Materials, University of Groningen, 9747 AG Groningen, The Netherlands*

²⁾*Instituto de Nanociencia y Nanotecnología CNEA-CONICET, Centro Atómico Bariloche, Av. E. Bustillo 9500, (R4802AGP) S. C. de Bariloche, Río Negro, Argentina*

³⁾*Instituto Balseiro, Universidad Nacional de Cuyo - CNEA, Av. Bustillo 9500, R8402AGP, S. C. de Bariloche, Río Negro, Argentina*

⁴⁾*Laboratoire de Physique des Solides, Université Paris-Sud, Université Paris-Saclay, CNRS, UMR8502, 91405 Orsay, France*

⁵⁾*Centro de Micro- y Nanoelectrónica Del Bicentenario, Instituto Nacional de Tecnología Industrial, Av. Gral Paz 5445, San Martín Buenos Aires, B1650KNA, Argentina*

⁶⁾*ECyT - CONICET, Universidad de San Martín, Av. 25 de Mayo y Francia (1650) San Martín, Argentina*

⁷⁾*ECyT, Universidad de San Martín, Av. 25 de Mayo y Francia (1650) San Martín, Argentina*

⁸⁾*Departamento de Energía Solar, Centro Atómico Constituyentes (CNEA), Av. Gral Paz 1499, San Martín (Buenos Aires), Argentina*

(Dated: 14 October 2022)

Understanding and controlling the fabrication conditions of stacks with perpendicular magnetic anisotropy is a mandatory issue in order to achieve a memory device based on such principle. In that sense, the present work intends to demonstrate how the structural differences obtained by systematically varying the growth conditions may affect domain wall motion. Dealing with one prototypical system, such as Pt/Co/Pt, we have found that the magnetic properties, in particular the domain wall velocity, exhibit differences depending on substrate quality, magnetic layer thickness, and deposition atmosphere. Magneto-optical Kerr effect-based magnetometry and microscopy combined with X-ray reflectometry, atomic force microscopy and transmission electron microscopy were adopted as experimental techniques in order to elucidate the effect of growth conditions on domain wall dynamics.

Keywords: Perpendicular magnetic anisotropy, domain wall motion, sputtered Pt/Co/Pt, Magneto-optical Kerr effect

I. INTRODUCTION

Perpendicular magnetization is a remarkable property of some ferromagnetic films. It is a well-known phenomenon that occurs when the perpendicular magnetic anisotropy (PMA) is the dominant term among the competing magnetization dependent energy contributions¹. Systems with strong PMA that present out-of-plane magnetization offer better scale-down capacity and require lower current to induce magnetization switching, among other advantages for spintronics applications².

^{a)}Electronic mail: cpquinterosdominguez@gmail.com

Pt/Co/Pt is a prototypical system in which PMA was early observed and the magnetic domain wall (DW) motion discussed³. Since then, a large number of works have reported on how to induce PMA or improve its strength, by controlling different deposition parameters in Co/Pt based samples. Some authors have studied the correlation between the PMA and the microstructure of Co/Pt multilayers (ML) deposited on top of different buffer layers^{4,5}. Other authors have studied the effects of varying the Co thickness⁶ and the Pt thickness^{7,8}, as well as the effect of performing different annealing treatments⁹. In Pt/Co/Pt simple stacks deposited on different substrates, irradiation with He ions has proved to modify the PMA¹⁰. Moreover, Co-based simple stacks continue to be at the focus of intense research activity since the renewed interest on the Dzyaloshinskii-Moriya interaction¹¹. In this regard, recent studies of domain expansion under in-plane field in sputtered Pt/Co/Pt, have demonstrated the relevance of modifying the interfaces by controlling the deposition conditions. The Ar pressure during the deposition of the top Pt layer¹², the base pressure in the deposition chamber and the substrate temperature¹³ were shown to have an impact on the strength of the PMA and in the asymmetric velocity of magnetic bubble expansion under in-plane applied magnetic field. Also the effects of varying the thickness of the Co^{14,15} and the Pt^{15,16} layers on the DW velocity have been studied.

The magnetic properties (PMA and DW velocity) of Pt/Co/Pt samples used in the above mentioned studies have proved to be very sensitive to the deposition parameters. In fact, the precise deposition conditions may not be reproducible in different deposition systems¹², so that reporting on general trends turns to be more useful than paying attention to the precise parameters (base and deposition pressures, substrate temperature, substrate-to-target distance, layers thicknesses, etc.), when comparing samples from different groups. Within this framework, in this study we contribute to clarifying the role of some deposition conditions on the properties of Pt/Co/Pt films, mainly through the domain wall propagation analysis. We assess the impact of the substrate quality, Co thickness and base pressure in the deposition chamber on DW propagation velocity and correlate it with coercive field measurements. We pay particular attention on how these quantities depend on different deposition parameters and evaluate how the substrates and growth conditions are linked with magnetic domains nucleation and domain wall propagation processes.

II. SAMPLES: FABRICATION AND STRUCTURAL CHARACTERIZATION

Pt/Co/Pt films were deposited by dc magnetron sputtering at room temperature in a $(2.8 \pm 0.1) \times 10^{-3}$ Torr Ar atmosphere. The base pressure in the chamber prior to deposition was $\lesssim 10^{-6}$ Torr, unless indicated otherwise. Pt and Co targets were sputtered with 20 W and 10 W, respectively. The deposition rates were (1.25 ± 0.05) Å/s for platinum and (0.38 ± 0.08) Å/s for cobalt, for a distance from substrate to target of 86 mm. The trilayers studied in this work typically consist of Pt(8 nm)/Co(d_{Co})/Pt(4 nm) with d_{Co} ranging between 0.4 and 0.7 nm. Four different substrates were used in this work. Two of them are (001) oriented Si wafers from different manufacturers and different production years (i.e., different aging times): MTI®, 1998 (S1) and Crystal®, 2012 (S2). Although they are nominally the same material, they differ in their surface topography. We also used (001) oriented SrTiO₃ (STO) and thermally oxidized S1 with a 100 nm thick SiO₂ layer (SiO₂).

Systematic studies of the structural properties and domain wall propagation were performed on three batches of samples:

Series A: different substrates. Pt/Co/Pt trilayers deposited on three different substrates: silicon (S2), STO and SiO₂. The deposition time for Co was $t_{Co} = 18$ s and the base pressure ranged between 6.7 and 7.3×10^{-7} Torr.

Series B: different Co thicknesses. Pt/Co(t_{Co})/Pt samples with varying Co deposition times ($t_{Co} = 12, 15$ and 18 s), which resulted in different Co thicknesses (d_{Co}). This series was deposited on S1 substrates. The base pressure ranged between 9.0 and 9.3×10^{-7} Torr.

Series C: different base pressures. Pt/Co/Pt trilayers deposited on S1 substrates with $t_{\text{Co}} = 15$ s using 3×10^{-6} and 1×10^{-5} Torr base pressures in the sputtering chamber before the deposition procedure. Since the deposition takes place with the same Ar pressure as the other series, we assume that the initial base pressure may affect the cleanness of the environment rather than the growth dynamics.

Transmission electron microscopy (TEM) images were acquired with a Philips CM200 microscope using an acceleration voltage of 200 keV. Samples for TEM observations were prepared by focused ion beam (FIB) with a FEI Helios Nanolab 650 dual beam system. A lamella was extracted from the bulk sample by ion milling and then transported to a copper grid with micromanipulators, where it was fixed at its final position with a local Pt deposition. The lamella was then thinned to sub-100 nm thickness and a final cleaning process was performed with 5 kV ion beam acceleration voltage.

Figure 1 shows TEM images of a Pt/Co/Pt lamella. Since the contrast is related to the atomic mass, Co can be distinguished in Fig. 1(a) as a brighter stripe between the two dark Pt layers. The Si substrate and its native oxide layer are indicated. On top of the trilayer, granular Pt deposited during the FIB processing can be recognized. Continuity of the Co film was observed along the whole extension of the lamella. This observation allows us to rule out all possible effects coming from discontinuities of the Co layer¹⁷. Complementarily, Figure 1(b) shows that the trilayer copies the topographical defects of the substrate: a bump is observed in both the film and the substrate. The dark portion of the image corresponds to the Pt/Co/Pt stack, the Co layer being hardly visible in this magnification. The bump on the substrate is distinguished as a brighter region within the dark gray of the Pt/Co/Pt film, indicated with a dashed line.

To further analyze to which extent the substrate topography affects the film quality, atomic force microscopy (AFM) images were acquired for each substrate and corresponding film. Measurements were conducted in tapping mode with a Veeco Dimension 3100 NanoScope. AFM images are presented in Fig. 2 for the different substrates [panels (a)-(d)] and Pt/Co/Pt trilayers deposited on each of them [panels (e)-(h), respectively]. For different substrates, different density of defects and roughnesses were observed. To quantify the roughness, Rq (the RMS deviation from the average plane) was computed for $(2 \mu\text{m})^2$ selected areas. The images in Fig. 2 are ordered by increasing roughness from left to right. It is interesting to compare both (001) Si wafers with native oxide, S1 and S2: although they are nominally the same material, their surface topographies are noticeably different, as discussed in a previous work¹⁸. The SiO_2 substrate, obtained by thermally oxidizing a S1 wafer, presents a reduced roughness after the process. Figure 2 shows that the Pt/Co/Pt trilayers reproduce the topography of the substrates beneath, as suggested by TEM observations.

X-ray reflectivity (XRR) experiments were performed with $\text{Cu-K}\alpha$ radiation ($\lambda = 1.54 \text{ \AA}$) using an Empyrean PANalytical System. Figure 3(a) shows experimental data for a trilayer with total thickness of 13.13 nm deposited on S1 substrate. The periodicity of the oscillations (Kiessig fringes) in the XRR curves is determined by the total thickness of the sample¹⁹. When the electronic density of the film is higher than that of the substrate, as in the present case, the total thickness d of the film is related to the angular positions of the minima θ_m through the modified Bragg law²⁰

$$\sin^2 \theta_m = 2\delta + m^2(\lambda/2d)^2, \quad (1)$$

where $1 - \delta$ is the real part of the refractive index of the film and m the order of each minimum, indicated in Fig. 3(a). The inset of Fig. 3(a) shows the relationship between $\sin^2 \theta_m$ and m^2 ; the total thickness d of the sample is obtained from the slope of the linear fit to the experimental data, by using Eq. (1). This procedure was employed to measure the total thickness of all the studied samples, the results are displayed in Fig. 3(b)-(d). Our deposition method gives a 10 % dispersion in the measured total thickness, when

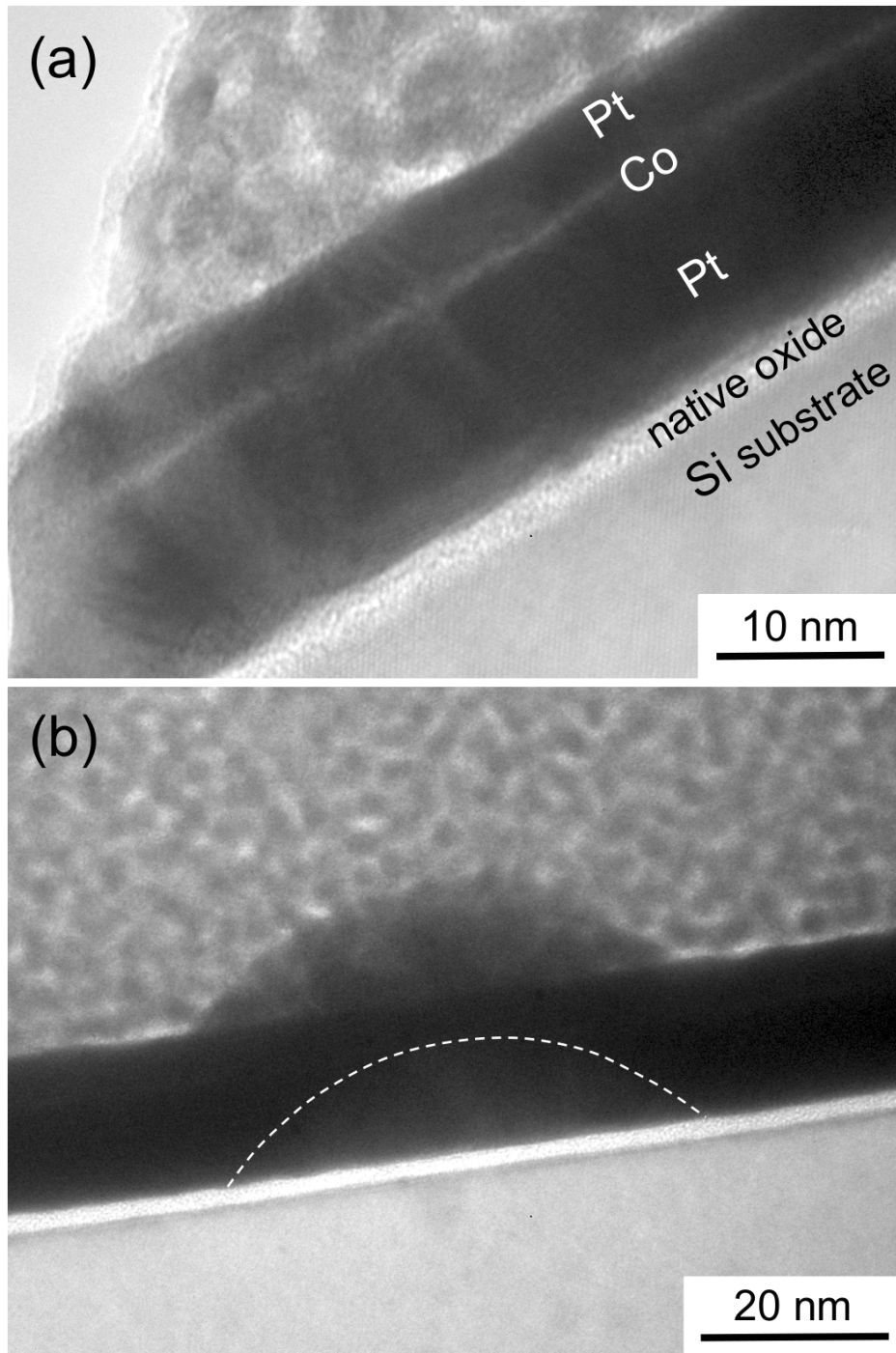


FIG. 1. Transmission electron microscopy images of a lamella of a Pt/Co/Pt film on a Si substrate prepared with focused ion beam. (a) Continuity of the Co layer is demonstrated. (b) The trilayer copies the topography of the substrate, a bump is shown as an example. The dashed line is a guide to the eye, delimiting the brighter region identified as a bump on the substrate.

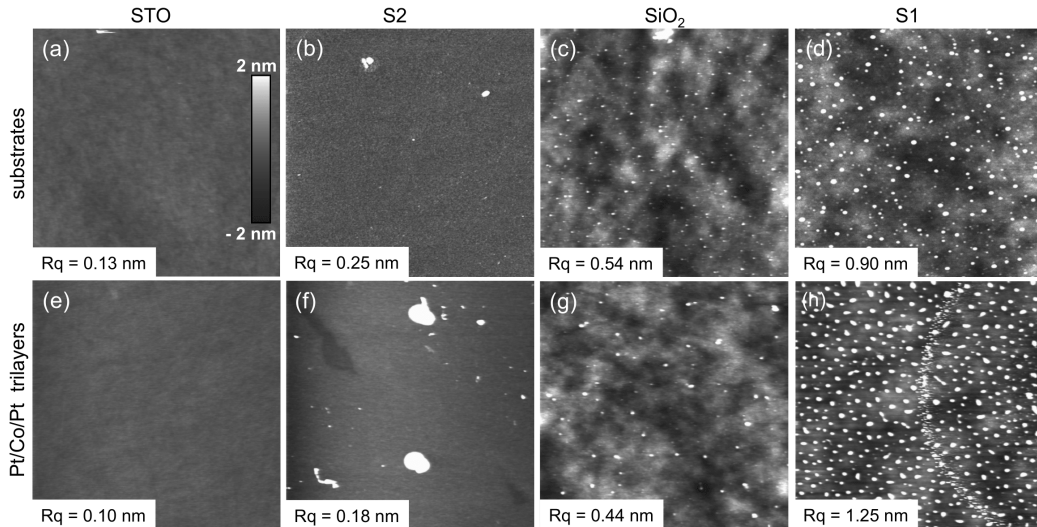


FIG. 2. Atomic force microscopy images of the surface topography. Above: the substrates STO (a), S2 (b), SiO_2 (c) and S1 (d). Below, (e)-(h): Pt/Co/Pt trilayers selected from Series A and B, with the same Co thickness ($d_{\text{Co}} = 0.64$) nm, deposited over the different substrates. All the images have $5 \mu\text{m} \times 5 \mu\text{m}$ area and are displayed in the same gray scale, with 4 nm amplitude. The roughness Rq was computed using a $(2 \mu\text{m})^2$ selected area from each sample. In the case of the trilayer on S2 (f), the big defects were intentionally avoided for the computation of Rq . Reproduced from Appl. Phys. Lett. 112, 262402 (2018), with the permission of AIP Publishing.

comparing samples with the same deposition times but from different batches. Since the Co thickness d_{Co} is one of the relevant parameters which influences the magnetic properties we intend to study, we carefully estimated this quantity for each trilayer. In order to compute d_{Co} , we used previously calibrated deposition rates of $r_{\text{Pt}} = (1.25 \pm 0.05) \text{ \AA/s}$ for Pt and $r_{\text{Co}} = (0.38 \pm 0.08) \text{ \AA/s}$ for Co, and we assumed that the ratio R between those rates remains unchanged with a value $R = r_{\text{Pt}}/r_{\text{Co}} = 3.3 \pm 0.4$. Under that assumption, knowing the deposition times t_{Pt} and t_{Co} for each single layer and using the experimental total thicknesses d presented in Fig. 3(b)-(d), we estimated the Co thickness d_{Co} for each sample as

$$d_{\text{Co}} = \frac{t_{\text{Co}} d}{t_{\text{Co}} + R t_{\text{Pt}}}. \quad (2)$$

The results, presented in Fig. 3(e)-(g), confirm that while Series B has varying t_{Co} , Series A and Series C trilayers have the same Co thickness within each series. Thus, we can state that any effects due to varying Co thickness will only be observed within Series B.

III. DOMAIN WALL MOTION

The films studied in this work present out-of-plane magnetization, which is demonstrated by the squared magnetization loops obtained when the magnetic field is applied perpendicular to the sample. Magneto-optical Kerr effect (MOKE) magnetometry in the polar configuration was used to measure out-of-plane magnetization loops. The experimental curves presented in Fig.4 were acquired with a magnetic field sweeping rate of 220 Oe/s.

The magnetic-field-driven domain wall (DW) motion was studied in a home-made MOKE microscope in the polar configuration (PMOKE). The most relevant features of the used microscope are the *Olympus LMPLFLN* series objectives (20 \times and 5 \times), a high-brightness

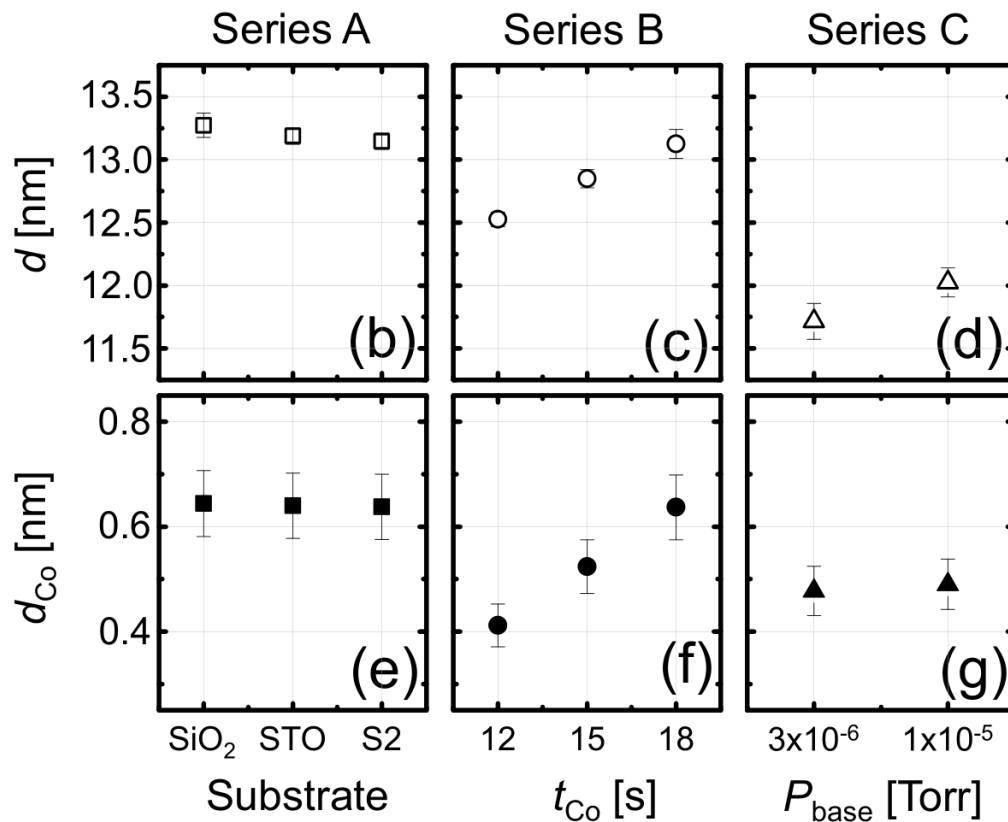
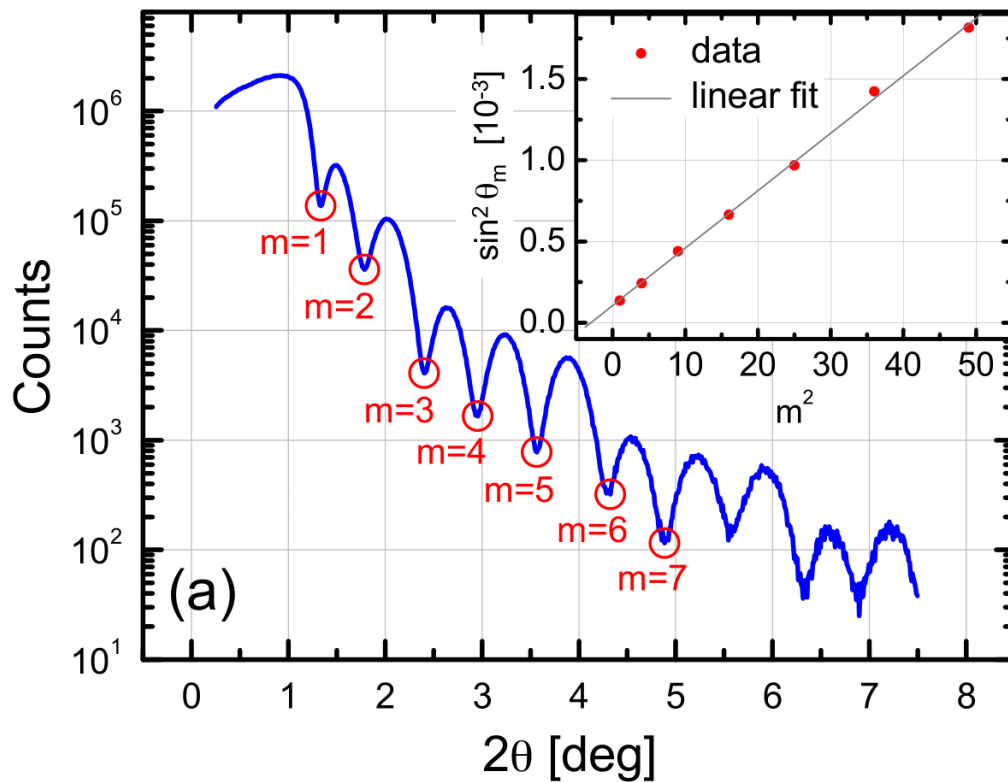


FIG. 3. (a) X-ray reflectivity of a Pt/Co/Pt sample with $t_{Co} = 18$ s deposited on S1 substrate (Series B). The angular positions of the minima are indexed. The inset shows $\sin^2 \theta_m$ vs. m^2 (being θ_m the angles for XRR minima and m the index of each minimum). The line is a linear fit to the experimental data; the slope is used to compute the total thickness of the samples by means of Eq. (1). The total thicknesses for samples with (b) different substrates, (c) different Co thicknesses and (d) different base pressures are presented. The respective Co thicknesses, displayed in (e)-(g), were estimated using Eq. (2) as described in the text.

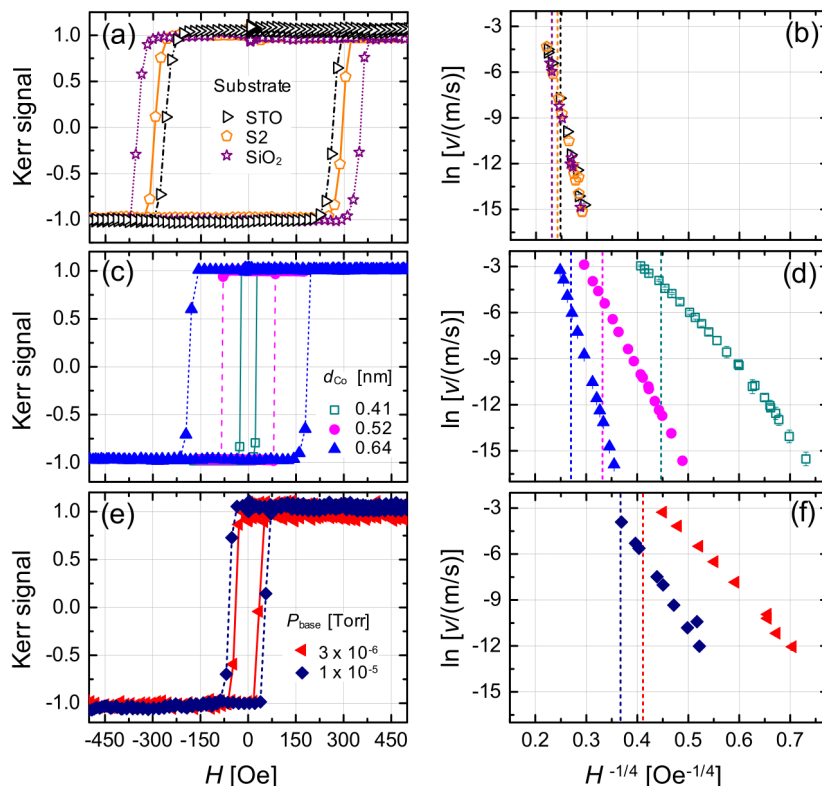


FIG. 4. Normalized magnetization loops obtained by Kerr magnetometry [(a),(c) and (e)] and DW velocity curves displayed as $\ln v$ vs. $H^{-1/4}$ [(b),(d) and (f)] grouped by series of samples; the vertical dashed lines indicate the coercive field obtained from the magnetization loop of each sample. All the measurements were carried out at room temperature. (a) Magnetization loops and (b) DW velocity for **Series A**: Pt/Co/Pt films deposited on different substrates, with $d_{\text{Co}} = (0.64 \pm 0.06)$ nm and base pressure before deposition $P_{\text{base}} = (7.1 \pm 0.2) \times 10^{-7}$ Torr. (c) Magnetization loops and (d) DW velocity for **Series B**: samples with different d_{Co} deposited over S1 substrates with $P_{\text{base}} = (9.1 \pm 0.2) \times 10^{-7}$ Torr. (e) Magnetization loops and (f) DW velocity curves for **Series C**: samples deposited with different P_{base} on S1 substrates with cobalt thickness $d_{\text{Co}} = (0.48 \pm 0.05)$ nm. Reproduced from Appl. Phys. Lett. 112, 262402 (2018), with the permission of AIP Publishing.

red LED with a dominant wavelength 637 nm, two Glan-Thompson polarizers, a 14 bit CCD from *QImaging Corp.* and the illumination set in a Köhler configuration. PMOKE microscopy images consist of regions with two different gray levels, that correspond to magnetic domains with the magnetization pointing in opposite directions perpendicular to the sample plane. Due to the weak magnetic contrast in a typical PMOKE image of the studied samples, it is better to work with differential images. Either an image of the saturated sample is subtracted as a background, or consecutive micrographs are subtracted from each other. The acquisition and analysis procedures followed in this work are described in detail in Ref. [18]. The sample is first saturated and then a magnetic field pulse with the opposite polarity is applied to produce domain nucleation. In order to study the DW dynamics, a series of square magnetic field pulses of intensity H and duration Δt are applied and PMOKE images are acquired after each pulse. The DW velocity is computed as $v = \Delta x / \Delta t$, where Δx is the distance traveled by the DW between consecutive images. By reproducing this procedure for different magnetic field intensities, we obtain $v(H)$ curves. In the present work, the DW velocity curves are presented as $\ln v$ vs. $H^{-1/4}$ plots. The fact that these curves present a linear behavior is compatible with the DW movement taking place within the creep regime^{3,21–23}.

In the following, we present a study of the variations in the room-temperature DW velocity and coercive field produced by changing either the substrate (Series A), the Co thickness (Series B) or the base pressure in the deposition chamber (Series C). We have evaluated the degree of reproducibility of our samples, and we have confirmed that the variations in DW velocity vs. magnetic field described below are larger than the dispersion due to reproducibility limitations, as long as we compare samples from the same series.

Room temperature magnetization loops presented in Fig. 4(a) evidence a variation of the coercive field in samples of Series A. In addition, Fig. 4(b) compares the DW velocity for the same batch. The three samples present roughly the same $\ln v$ vs. $H^{-1/4}$ curves. The coercive field of Pt/Co/Pt films increases with increasing roughness, while the DW velocity curves do not evidence any dependence on the topography of the samples.

Magnetization loops in Fig. 4(c) (Series B) show that the coercive field increases with increasing thickness, as observed previously by Metaxas *et al.*¹⁴. Fig. 4(d) demonstrates that DW velocity changes dramatically with the Co thickness: the DW velocity at 15 Oe is $2.5 \cdot 10^{-3}$ m/s for the $d_{\text{Co}} = 0.41$ nm sample against $1.1 \cdot 10^{-7}$ m/s for the $d_{\text{Co}} = 0.52$ nm sample. Additionally, the smaller the coercive field is, the faster the DWs move.

Two different base pressures were used in order to analyze the impact of this parameter on DW motion (Series C). Figures 4(e) and (f) show the coercive field and DW velocity dependence on such parameter. Even though both of the used base pressures are orders of magnitude lower than the Ar pressure required for plasma ignition, DW motion is strongly affected by the initial condition of the deposition process. In fact, the DW velocity is higher in the case of a cleaner environment before the introduction of Ar. If we choose a fixed field value (e.g. 16 Oe), velocities of $4.1 \cdot 10^{-3}$ m/s for $3 \cdot 10^{-6}$ Torr and $2.8 \cdot 10^{-5}$ m/s for $1 \cdot 10^{-5}$ Torr are found. The DW velocity is more sensitive to changes in the base pressure than the coercive field.

IV. DISCUSSION AND CONCLUSIONS

The impact of deposition conditions on DW dynamics was studied in Pt/Co/Pt stacks with perpendicular magnetization deposited by dc sputtering. We studied samples from three batches, each of them varying a different deposition parameter: changing the substrates roughness (Series A), varying Co thickness (Series B) and modifying the base pressure in the deposition chamber (Series C).

In a previous work, we detected a noticeable difference in DW dynamics between samples deposited on nominally equal (001) Si substrates with native oxide presenting different surface topographies¹⁸. In order to further study the impact of roughness on the properties of the films, in the present work we analyzed a batch of samples deposited on three different substrates: (001) Si wafer, thermally oxidized (001) Si and (001) SrTiO₃. Since the structural characterization performed by TEM and AFM confirmed that the films reproduce the topography of the substrate surface, by changing the substrate we obtained Pt/Co/Pt films with the same Co thickness and different roughness values. We found an increasing tendency of the coercive fields with increasing roughness. On the contrary, the DW velocity has roughly the same behaviour with magnetic field for all the samples. The trend observed within Series A seems to point that not only the nature of the substrate but also the topographical landscape has an impact on the magnetization reversal. In particular, this would imply that different buffer layers might be playing a differential role depending on their roughnesses⁴⁻⁸. On the contrary, the DW propagation dynamics under an applied magnetic field is the same for all these samples throughout the studied field range. This indicates that once the nucleation is promoted the DW propagation remains the same regardless of the quality of the surface. It is worth to mention that the variation of velocity curves reported in a previous work by some of us¹⁸ was somewhat misleading since we compared samples from different batches, as we were not aware at that time of the degree of sensitivity of DW velocity to subtle variations in the deposition conditions.

Regarding Series B, it was shown that Co thickness is strongly determinant for both the

coercive field and the DW velocity. In particular, the increase of the coercive field with the Co thickness is in agreement with the work from Metaxas *et al.*¹⁴ on Pt/Co/Pt, and opposite to what Su *et al.*²⁴ obtained for Co/Ni stacks.

Finally, we have assessed the changes in DW motion due to base pressure modification (Series C). We have observed that the coercive field is not so sensitive to slight variations in the base pressure. However, a cleaner environment prior to sample deposition leads to noticeably higher DW velocity. This indicates that not only Ar pressure during deposition is relevant to determine the properties of the obtained material^{5,12,25}, but also the base pressure prior to deposition, since it defines the degree of gas purity within the chamber and may strongly affect also the purity of the obtained materials.

It is worth noticing that the coercive field H_C is mainly associated to the nucleation of magnetic domains. This is supported by the fact that the DW velocity at the coercive field is rather high, as demonstrated in Fig. 4; so, once the domains are nucleated at H_C , the DWs undergo fast propagation. On the other hand, the DW velocity comprises only the DW propagation processes, as determined by the experimental conditions. This suggests that the main impact of changing the substrate, i.e. changing the roughness of the samples, is on the nucleation process, while the DW propagation is roughly insensitive to the surface topography. The opposite is observed when changing the base pressure in the deposition chamber, thus modifying the purity of the materials at the atomic level, which strongly affects the DW propagation process, but not so much the domains nucleation. The Co thickness is a relevant parameter for both kinds of processes, equally affecting domain nucleation and DW propagation.

Further studies are necessary in order to clarify the source of these differences. Nevertheless, one might speculate on whether this differential impact may arise from the scale of the domain wall width and how it compares to the size of the defects of different nature (impurities coming from the cleanness of the chamber vs topographical texture). However, other effects might need to be considered. Among them, we can mention the suppressed domain nucleation Emori *et al.*⁵ have reported when comparing Pt and Ta or TaO_x buffered Co/Pt MLs. In that case, they explained this suppression by means of an enhanced film quality in favor of the Pt-buffered MLs.

To conclude, we have studied the impact of the samples roughness, Co thickness and base pressure on the coercive field, associated to domains nucleation, and on the DW velocity, associated to domain wall propagation. The information provided here could allow for tuning at will the coercive field and DW velocity of Pt/Co/Pt samples for particular applications, by choosing an appropriate combination of deposition parameters. This work also contributes to shed light onto the wide dispersion of magnetic properties, in particular DW velocity, of apparently equivalent samples: DW velocity turns out to be extremely sensitive to slight changes in some deposition parameters (e.g., base pressure and Co thickness), even when comparing samples grown in the same deposition system.

ACKNOWLEDGMENTS

We acknowledge grants from Agencia Nacional de Promoción Científica y Tecnológica (PICT 2014-2237, PICT 2016-0069, PICT 2017-0906) and Universidad Nacional de Cuyo (UNCuyo 06/C561).

¹F. J. A. der Broeder, W. Hoving, and P. J. H. Bloemen, “Magnetic anisotropy of multilayers,” *J. Magn. Mater.* **93**, 562–570 (1991).

²B. Dieny and M. Chshiev, “Perpendicular magnetic anisotropy at transition metal/oxide interfaces and applications,” *Rev. Mod. Phys.* **89**, 025008 (2017).

³S. Lemerle, J. Ferré, C. Chappert, V. Mathet, T. Giamarchi, and P. Le Doussal, “Domain wall creep in an ising ultrathin magnetic film,” *Phys. Rev. Lett.* **80**, 849–852 (1998).

⁴J. Kanak, M. Czapkiewicz, T. Stobiecki, M. Kachel, I. Sveklo, A. Maziewski, and S. v. Dijken, “Influence of buffer layers on the texture and magnetic properties of Co/Pt multilayers with perpendicular anisotropy,” *Phys. Status Solidi (a)* **204**, 3950–3953 (2007).

⁵S. Emori and G. S. D. Beach, “Optimization of out-of-plane magnetized Co/Pt multilayers with resistive buffer layers,” *J. App. Phys.* **110**, 033919 (2011).

- ⁶P. Chowdhury, P. D. Kulkarni, M. Krishnan, H. C. Barshilia, A. Sagdeo, S. K. Rai, G. S. Lodha, and D. V. Sridhara Rao, “Effect of coherent to incoherent structural transition on magnetic anisotropy in Co/Pt multilayers,” *J. Appl. Phys.* **112**, 023912 (2012).
- ⁷S. T. Lim, M. Tran, J. W. Chenchen, J. F. Ying, and G. Han, “Effect of different seed layers with varying Co and Pt thicknesses on the magnetic properties of Co/Pt multilayers,” *J. Appl. Phys.* **117**, 17A731 (2015).
- ⁸M. Bersweiler, K. Dumesnil, D. Lacour, and M. Hehn, “Impact of buffer layer and Pt thickness on the interface structure and magnetic properties in (Co/Pt) multilayers,” *J. Phys.: Condens. Matter* **28**, 336005 (2016).
- ⁹T. Y. Lee, Y. Chan Won, D. Su Son, S. Ho Lim, and S.-R. Lee, “Effects of Co layer thickness and annealing temperature on the magnetic properties of inverted [Pt/Co] multilayers,” *J. Appl. Phys.* **114**, 173909 (2013).
- ¹⁰J. Ferré, C. Chappert, H. Bernas, J.-P. Jamet, P. Meyer, O. Kaitasov, S. Lemerle, V. Mathet, F. Rousseaux, and H. Launois, “Irradiation induced effects on magnetic properties of Pt/Co/Pt ultrathin films,” *J. Magn.Magn. Mater.* **198-199**, 191–193 (1999).
- ¹¹A. Fert, N. Reyren, and V. Cros, “Magnetic skyrmions: advances in physics and potential applications,” *Nat. Rev. Mater.* **2**, 17031 (2017).
- ¹²R. Lavrijsen, D. M. F. Hartmann, A. van der Brink, Y. Yin, B. Barcones, R. A. Duine, M. A. Verheijen, H. J. M. Swagten, and B. Koopmans, “Asymmetric magnetic bubble expansion under in-plane field in Pt/Co/Pt: Effect of interface engineering,” *Phys. Rev. B* **91**, 104414 (2015).
- ¹³A. W. J. Wells, P. M. Shepley, C. H. Marrows, and T. Moore, “Effect of interfacial intermixing on the Dzyaloshinskii-Moriya interaction in Pt/Co/Pt,” *Phys. Rev. B* **95**, 054428 (2017).
- ¹⁴P. J. Metaxas, J. P. Jamet, A. Mougín, M. Cormier, J. Ferré, V. Baltz, B. Rodmacq, B. Dieny, and R. L. Stamps, “Creep and flow regimes of magnetic domain-wall motion in ultrathin Pt/Co/Pt films with perpendicular anisotropy,” *Phys. Rev. Lett.* **99**, 217208 (2007).
- ¹⁵E. Jué, C. K. Safeer, M. Drouard, A. Lopez, P. Balint, L. Buda-Prejbeanu, O. Boulle, S. Auffret, A. Schul, A. Manchon, I. M. Miron, and G. Gaudin, “Chiral damping of magnetic domain walls,” *Nat. Mater.* **15**, 272–277 (2015).
- ¹⁶S.-G. Je, D.-H. Kim, S.-C. Yoo, B.-C. Min, K.-J. Lee, and S.-B. Choe, “Asymmetric magnetic domain-wall motion by the Dzyaloshinskii-Moriya interaction,” *Phys. Rev. B* **88**, 214401 (2013).
- ¹⁷M. Charilaou, C. Bordel, P.-E. Berche, B. B. Maranville, P. Fischer, and F. Hellman, “Magnetic properties of ultrathin discontinuous Co/Pt multilayers: Comparison with short-range ordered and isotropic CoPt₃ films,” *Phys. Rev. B* **93**, 224408 (2016).
- ¹⁸C. P. Quinteros, S. Bustingorry, J. Curiale, and M. Granada, “Correlation between domain wall creep parameters of thin ferromagnetic films,” *Appl. Phys. Lett.* **112**, 262402 (2018).
- ¹⁹V. Holý, U. Pietsch, and T. Baumbach, *High-Resolution X-Ray Scattering from Thin Films and Multilayers* (Springer-Verlag, 1999).
- ²⁰O. Nakamura, E. E. Fullerton, J. Guimpel, and I. K. Schuller, “High T_C thin films with roughness smaller than one unit cell,” *Appl. Phys. Lett.* **60**, 120 (1992).
- ²¹T. Nattermann, “Scaling approach to pinning: Charge density waves and giant flux creep in superconductors,” *Phys. Rev. Lett.* **64**, 2454–2457 (1990).
- ²²P. Chauve, T. Giamarchi, and P. Le Doussal, “Creep and depinning in disordered media,” *Phys. Rev. B* **62**, 6241–6267 (2000).
- ²³V. Jeudy, A. Mougín, S. Bustingorry, W. Savero Torres, J. Gorchon, A. B. Kolton, A. Lemaître, and J.-P. Jamet, “Universal pinning energy barrier for driven domain walls in thin ferromagnetic films,” *Phys. Rev. Lett.* **117**, 057201 (2016).
- ²⁴X. Su, T. Jin, Y. Wang, Y. Ren, L. Wang, J. Bai, and J. Cao, “Evolution of magnetic properties and domain structures in Co/Ni multilayers,” *Jpn. J. Appl. Phys.* **55**, 110306 (2016).
- ²⁵K.-W. Park, Y.-W. Oh, D.-H. Kim, J.-Y. Kim, and B.-G. Park, “Effect of sputtering pressure on stacking fault density and perpendicular magnetic anisotropy of CoPt alloys,” *J. Phys. D: Appl. Phys.* **49**, 345002 (2016).